ROYAL SOCIETY
OF CHEMISTRY

Dangerous liaisons: anion-induced protonation in phosphate–polyamine interactions and their implications for the charge states of biologically relevant surfaces†

Gregorio Laucirica, Waldemar A. Marmisollé* and Omar Azzaroni

Although not always considered a preponderant interaction, amine–phosphate interactions are omnipresent in multiple chemical and biological systems. This study aims to answer questions that are still pending about their nature and consequences. We focus on the description of the charge state as surface charges constitute directing agents of the interaction of amine groups with either natural or synthetic counterparts. Our results allow us to quantitatively determine the relative affinities of HPO_4^{2-} and $H_2PO_4^-$ from the analysis of the influence of phosphates on the zeta-potential of amino-functionalized surfaces in a broad pH range. We show that phosphate anions enhance the protonation of amino groups and, conversely, charged amines induce further proton dissociation of phosphates, yielding a complex dependence of the surface effective charge on the pH and phosphate concentration. We also demonstrate that phosphate–amine interaction is specific and the modulation of surface charge occurs in the physiological phosphate concentration range, emphasizing its biochemical and biotechnological relevance and the importance of considering this veiled association in both *in vivo* and *in vitro* studies.

Introduction

There is a large variety of biological systems in which a number of different complex chemical structures are assembled from simple building blocks by non-covalent interactions. The understanding of such kinds of systems not only provides fundamental knowledge about supramolecular interactions but also constitutes a source of inspiration for the rational design of new chemical architectures.[1–6]

In particular, electrostatic interactions largely dominate the behavior of charged species and this is the reason why surface charges are determinant in the interactions of proteins with biological counterparts or pharmaceutical products.[7–9] The same electrostatic interactions constitute a guide to perform the assembly of charged proteins on solid surfaces or with other artificial counterparts in the construction of a variety of biodevices.[10,11] This interplay of electrostatic charges translates not only into structural but also into functional consequences.[12–15] On the other hand, surface charges are also important in the regulation of other completely artificial systems, such as the

electrostatically driven layer-by-layer building up of polyelectrolytes and nanomaterials employed in diverse techniques of surface modification.[16]

Protonated amine groups are the more usual type of cationic moieties in biomolecules. According to the pH of the medium, the amine moieties could be protonated yielding a positive surface charge. However, these groups can also be associated with small anions that could modify their effective charge and, thus, their interactions with other counterparts. The specific adsorption of phosphate anions on self-assembled monolayers (SAMs) of amino-functionalized thiols[17] and layer-by-layer assemblies of polyallylamines[18] has been reported. In both cases, the experimental results indicate that some charge inversion occurs at physiological phosphate concentrations.[19] The normal serum phosphate concentration is about 1 mM,[20,21] but it can be higher in specific cell compartments; for example, the total phosphate concentration ranges from 4 mM (intracellular) to 16 mM (mitochondrial) in liver cells.[22] Thus, the understanding of the phenomena that determine the surface charges of amino surface groups in the presence of phosphates within the millimolar range becomes biochemically significant.

Additionally, the association of amines and phosphate anions plays a key role in the self-assembly of multiple biological supramolecular structures. Long-chain polyamines and silaffins (proteins with a high degree of phosphate and amine groups) constitute the main organic components of biosilica, and their

Instituto de Investigaciones Fisicoquímica Teóricas y Aplicadas (INIFTA), Departamento de Química, Facultad de Ciencias Exactas, Universidad Nacional de La Plata (UNLP), CONICET. 64 and 113, La Plata, Argentina. E-mail: wmarmi@inifta.unlp.edu.ar

phosphate/amine aggregates are considered to be the primers of specific mineral domains in diatoms.[23,24] Other examples of supramolecular association of biogenic polyamines and phosphate ions are the nuclear aggregates of polyamines (NAPs), which are present in many replicating cells,[25] acting as modulators of conformation and protectors of the DNA structure.[26] H-NMR studies indicate that ammonium cations are those interacting electrostatically with phosphate anions in the NAPs.[25,27] However, it has also been postulated that hydrogen-bond interactions are responsible for the tridimensional stabilization of the NAPs.[26]

Polyallylamine hydrochloride (PAH) has become a simple model of biological polyamine in diverse basic studies of amine/phosphate aggregation.[28,29] NMR studies indicate that electrostatic interactions between PAH and phosphates are present in the whole pH range in which amines are protonated. Phosphates produce aggregates more efficiently than other polyvalent anions and it has even been suggested that protonated amines induce an additional dissociation of phosphate anions.[30] Recently, it has been demonstrated that the aggregation of PAH and phosphates from solution can be employed for the reversible formation of films on different substrates, becoming an easily made simple building block for the design and construction of supramacromolecular interfacial architectures.[31] Furthermore, dimers and trimers of phosphates can induce the formation of initial aggregates which then yield macroscopic gels on both hydrophobic and hydrophilic substrates.[32,33]

The specific affinity between soluble polyamines and phosphate anions that yield these supramolecular aggregates also manifests itself when amino surface groups are exposed to phosphates in solution. With this background in mind, and due to the fact that polyamine–phosphate interactions are omnipresent in multiple chemical and biological systems, this study aims to answer the following – fundamental – still pending questions: Does the binding just depend on the valence of the anion? What are the relative affinities of singly and doubly charged phosphate anions? Does phosphate binding change the pK_a of amino groups? How relevant are H-bonding interactions to phosphate binding? Do counterions regulate protein adsorption beyond the traditional notion of electrostatic interactions?

In this work we study the binding of phosphate anions to amine groups employing silica microparticles capped by PAH as a simple model of the amino containing surface. We also develop a binding formalism to extract quantitative information from the dependence of the zeta-potential on the phosphate concentration at several pH values. We focus on the description of the charge state and the phenomenon of charge inversion as surface charges constitute "stalwart" directing agents of the interaction of amine groups with either natural or synthetic counterparts, with great biochemical and biotechnological implications. The specificity of the amine–phosphate interaction and the presence of different phosphate concentrations in a variety of cell compartments and biochemical media emphasize the importance of taking into account this binding equilibrium in both *in vivo* and *in vitro* studies.

Experimental

Chemicals

Polyallylamine hydrochloride (PAH) (*ca.* 58 kDa) was purchased from Sigma-Aldrich. The pH of stock solutions of PAH (1 mg mL^{-1}) was adjusted to 7 by adding 10% KOH. KH_2PO_4 and oxalic acid were from Carlo Erba, whereas K_2SO_4 was from Merck. Ethanol and NH_4OH were purchased from Anedra; tetraethyl orthosilicate (TEOS), HEPES, 3-mercapto-1-propanesulfonic acid sodium salt (MPS) and glucose oxidase (GOx) from *Aspergillus niger* were from Sigma-Aldrich.

All chemicals were of analytical grade. The water used in all experiments was purified using a Millipore system and its resistivity was 18.2 MΩ cm.

Preparation of silica particles

Silica particles (SPs) were synthesized using the Stöber method.[34] Briefly, 400 mL of ethanol and 110 mL of NH_4OH were mixed under magnetic stirring. Then 10 mL of TEOS was added, and the solution was stirred for 60 min at 60 °C. The reaction solution was then centrifuged to separate the SPs, which were successively re-dispersed and centrifuged twice employing ethanol and water as washing solvents.

For functionalization, the SPs were dispersed in 0.1 M KCl in 1 mg mL^{-1} PAH solution and stirred for 30 min to allow the adsorption of the polyelectrolyte. The SPs were then centrifuged and washed twice with 0.1 M KCl in 0.5 mM pH 7 HEPES buffer. These microparticles (MPs) will be referred to as SiO_2@PAH MPs.

Size and ζ-potential measurements

The size of the SPs was determined by DLS employing a Zetasizer Nano (Nano ZSizer-ZEN3600, Malvern, UK) in water at 25 °C employing a distribution fitting method. The size of the unmodified SPs was determined to be 250 ± 60 nm (see the ESI†).

The ζ-potential of the colloidal SPs was determined from the electrophoretic mobility measured by laser Doppler velocimetry with a Zetasizer Nano. The Smoluchowski approximation of the Henry equation was employed for calculations. Measurements were performed in triplicate using disposable capillary cells (DTS 1061 1070, Malvern) at 25 °C with a drive cell voltage of 30 V employing the monomodal analysis method.

Surface plasmon resonance spectroscopy (SPR)

Surface Plasmon Resonance (SPR) experiments were carried out using a SPR Navi 210A instrument (BioNavis Ltd, Tampere, Finland). An electrochemical flow cell (SPR321-EC, BioNavis Ltd) was employed for all measurements. Gold sensors (BioNavis Ltd) employed for SPR were soaked overnight in 10 mM MPS aqueous solution then rinsed with water and ethanol. Injection was performed manually and SPR angular scans (785 nm laser) were recorded with no flow in the cell. Temperature was maintained at 20 °C. All SPR experiments were processed using the BioNavis Data viewer software.

This journal is © the Owner Societies 2017

Phys. Chem. Chem. Phys., 2017, **19**, 8612–8620 | 8613

Glucose oxidase adsorption

The adsorption of GOx was monitored by SPR as the changes in the angle of minimum reflectivity can be correlated with the amount of adsorbed proteins on the gold substrates. The gold substrates were first modified by adsorbing a sulfonate-terminated thiol (MPS) and then allowing the adsorption of PAH under the same conditions as those employed for the functionalization of the SPs, by manually injecting the PAH solution and allowing the adsorption for 30 min before washing with 0.1 M KCl in 1 mM HEPES buffer, pH 7.4. Then, either the P_i-containing or P_i-free buffer was fluxed into the SPR cell for a few minutes to allow stabilization. The GOx solution (0.17 µM) in the corresponding buffer was then injected and the SPR angular scans were continuously recorded. After 25 minutes, a new injection of fresh buffer was performed to remove the non-bound protein.

Results and discussion

The zeta-potential (ζ) of SiO$_2$@PAH MPs depends strongly on the presence of phosphate anions as shown in Fig. 1(A). Independently of the pH of the solution, the addition of phosphate anions to 0.1 M KCl solution diminishes the value of the zeta-potential of the colloidal particles and it can even produce a charge inversion.
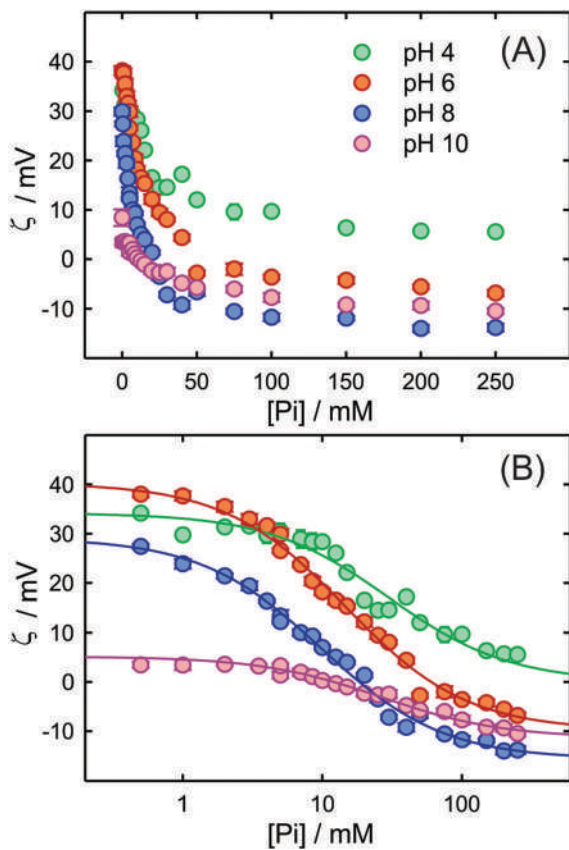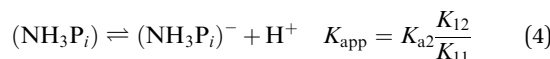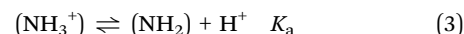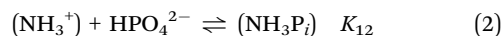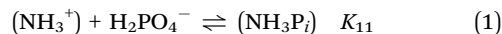

As the identity of the phosphate species depends on the pH, we use P_i to refer to the total inorganic phosphate.

The high salt concentration of the solutions employed prevents the initial changes, which could be attributed to changes in the ionic strength (all solutions were prepared in 0.1 M KCl) and it also provides the necessary conductivity for electrophoretic mobility measurements. We have also measured the effect of adding phosphates on the zeta-potential of bare SPs and no appreciable changes were observed in this case. These control experiments are presented in the ESI.†

The results in Fig. 1 reveal some kind of association between phosphate anions and charged surface groups. In the next section, we present a simple model to quantitatively analyze the zeta-potential data and their dependence on P_i concentration.
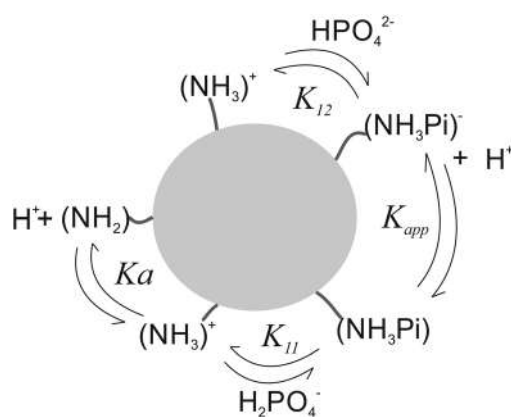
A. Phosphate binding to amine units

A.1.   Derivation of the model. Let us consider the binding equilibrium of the phosphate species to surface charged amino units. The main phosphate species in the range 4–10 are singly and doubly charged anions (see the ESI†). So, the only equilibriums we will consider for the quantitative analysis of the experimental data are those involving these species (Scheme 1). By assuming that the interaction is mainly electrostatically driven, we could consider the following association equilibriums (refer the ESI† for a detailed derivation of the model).

$$(NH_3{}^+) + H_2PO_4{}^- \rightleftharpoons (NH_3P_i) \quad K_{11} \tag{1}$$

$$(NH_3{}^+) + HPO_4{}^{2-} \rightleftharpoons (NH_3P_i) \quad K_{12} \tag{2}$$

$$(NH_3{}^+) \rightleftharpoons (NH_2) + H^+ \quad K_a \tag{3}$$

$$(NH_3P_i) \rightleftharpoons (NH_3P_i)^- + H^+ \quad K_{app} = K_{a2}\frac{K_{12}}{K_{11}} \tag{4}$$

where parentheses are used to designate surface species (see Scheme 1 for a summary of the involved equilibriums).

Zeta-potential being a measure of the surface charge, we will use the previous equilibriums to derive an expression for the surface charge in terms of the relative populations of amine moieties on the surface of the microparticles (Scheme 1). Owing to the binding equilibriums, these relative populations will in turn be

Fig. 1   Zeta-potential of the SiO$_2$@PAH microparticles as a function of the phosphate concentration in 0.1 KCl solutions of several adjusted pH values (A). Fittings of the values to eqn (14) (B).

Scheme 1   Summary of the main protonation and binding equilibriums considered for the quantitative model of phosphate binding to amine surface groups.

dependent on the phosphate bulk concentration, which is the key variable in our experiments.

Let Γ_{NH_2} be the total surface concentration of amino groups,

$$\Gamma_{NH_2} = [(NH_2)] + [(NH_3)^+] + [(NH_3P_i)] + [(NH_3P_i)^-] \tag{5}$$

We will use square brackets for surface concentrations of amino species. So, the notation [[( )]] will indicate the concentration of a surface-confined species. The exact meaning and units of this concentration are unimportant as we are interested in the relative populations at the end. We can use equilibriums (1)–(4) to reduce the number of amine species

$$\Gamma_{NH_2} = [(NH_3)^+]\left\{1 + \frac{[(NH_2)]}{[(NH_3)^+]} + K_B[P_i]\right\} \tag{6}$$

Here, we have defined the global constant for phosphate binding

$$K_B = K_{11}\alpha_1 + K_{12}\alpha_2 \tag{7}$$

where α_1 and α_2 are the bulk distribution functions of $H_2PO_4^-$ and HPO_4^{2-}, respectively, and simple Langmuir-type binding isotherms were considered for equilibriums (1) and (2). As before, $[P_i]$ refers to the bulk concentration of total phosphate species, which is the direct experimental variable in our experiments.

The changes in zeta-potential can be considered as resulting from changes of the relative populations of amine groups (no appreciable changes are observed in the hydrodynamic size of the microparticles due to phosphate concentration changes). In the present case, taking into account the charged surface species of the previous equilibriums, it is possible to write

$$\zeta \propto [(NH_3)^+] - [(NH_3P_i)^-] \tag{8}$$

which can be re-written as

$$\zeta \propto \Gamma_{NH_2}(1 - \alpha_- K_B[P_i])\left\{1 + \frac{[(NH_2)]}{[(NH_3)^+]} + K_B[P_i]\right\}^{-1} \tag{9}$$

where we have employed expression (6) and defined the fraction of dissociated adsorbed phosphate species

$$\alpha_- = [(NH_3P_i)^-]/([(NH_3P_i)] + [(NH_3P_i)^-]) \tag{10}$$

In the absence of binding anions, the zeta-potential becomes

$$\zeta_0 \propto \Gamma_{NH_2}\left\{1 + \frac{[(NH_2)]}{[(NH_3)^+]}\right\}^{-1} \tag{11}$$

This expression can be used to obtain the relative zeta-potential from eqn (9)

$$\zeta/\zeta_0 = \frac{(1 - \alpha_- K_B[P_i])}{\{1 + \theta_+ K_B[P_i]\}} \tag{12}$$

where we have defined

$$\theta_+ = \frac{[(NH_3)^+]}{[(NH_3)^+] + [(NH_2)]} \tag{13}$$

At this point it is important to note that neither eqn (12) nor parameters defined in eqn (10) and (13) depend on the absolute

concentration of surface amine species, but on relative populations. However, they do depend on pH through proton dissociation equilibriums (3) and (4).

Taking into account previous equations, the mathematical dependence of the zeta-potential on the phosphate bulk concentration ($[P_i]$) could be written as

$$\zeta = \zeta_0\frac{1 - A[P_i]}{1 + B[P_i]}, \tag{14}$$

where the parameters A and B are expected to have constant values at a given pH.

A.2. Evaluation of the model and fittings. Solid lines in Fig. 1 correspond to fittings of the experimental values to eqn (14). As shown in the figure (and the ESI†), the experimental results can be satisfactorily adjusted to the equation proposed by the simple binding model. The values of the parameters in eqn (14) were determined by non-linear fitting (*SigmaPlot*) and they are presented in Fig. 2 and 3. The extrapolated values of the experimental zeta-potentials at several pH values were fitted to the following equation (see Fig. 2)

$$\zeta_0 = \zeta_+\theta_+ = \zeta_+/(1 + 10^{n_o(pH-pK_a)}) \tag{15}$$

where the pK_a corresponds to the protonation equilibrium of the surface amino group (eqn (3)) and n_o was introduced to account for the pK_a distribution of the surface groups (see the ESI†). The determined values of pK_a and n_o were 8.7 ± 0.2 and 0.65 ± 0.2 respectively. The value of the effective pK_a of the surface amino groups is close to that reported for the solution pK_a of polyallylamine (8.5[35]–9.2[36]) reinforcing the physical meaning of the model. The shifting of the pK_a to lower values compared to the simple amines in solution and the spreading of the pK_a distribution (computed here by n_o) are consistent with the confinement caused by the attachment to the surface that hinders the protonation of amines close to protonated groups owing to the electrostatic repulsion.[37]

Expressions for A and B can be deduced from previous equations

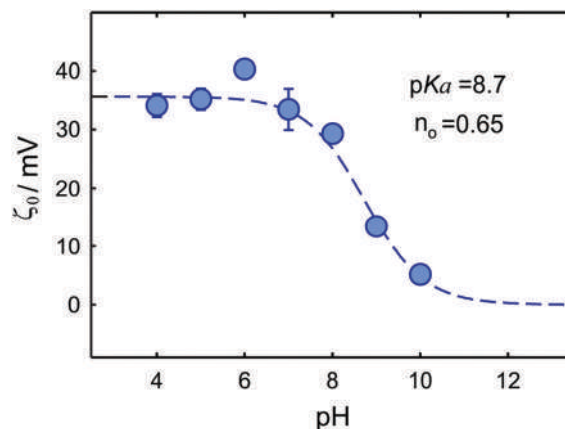$$A = (K_{11}\alpha_1 + K_{12}\alpha_2)/(1 + 10^{-n_{app}(pH-pK_{app})}) \tag{16}$$

Fig. 2 Extrapolated values of the zeta-potential of SiO₂@PAH microparticles at different pH values.

This journal is © the Owner Societies 2017

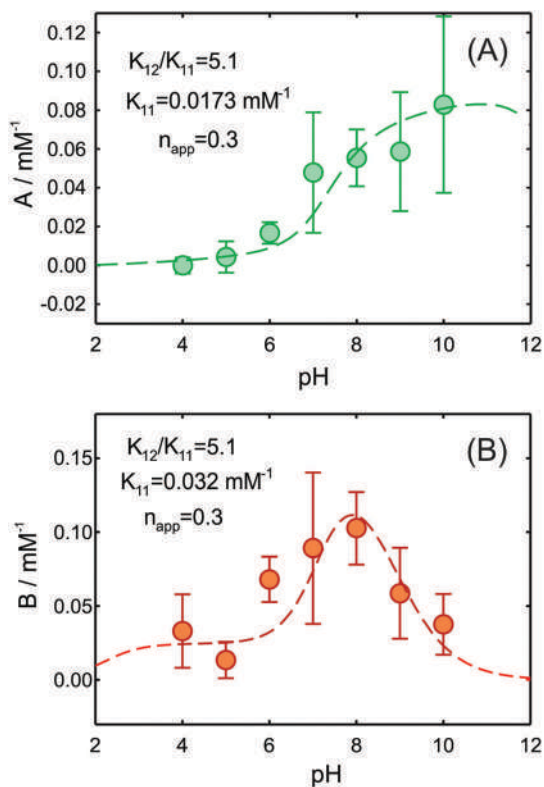*Phys. Chem. Chem. Phys.*, 2017, **19**, 8612–8620 | **8615**

Fig. 3 Values of parameters A and B in eqn (15) determined by non-linear fitting of experimental data in Fig. 1. Bars indicate the standard error of each parameter from the fittings.

where K_{app} was defined in eqn (4) and n_{app} was introduced to account for the wideness of the pK_a distribution of the binding equilibrium of the surface-bound phosphate groups.

$$B = (K_{11}\alpha_1 + K_{12}\alpha_2)/(1 + 10^{n_o(pH-pK_a)}) \quad (17)$$

From the fittings of ζ_0, the values of the parameters of the amine protonation were determined, so the values of K_{11}, K_{12}/K_{11} and n_{app} can be fitted from the pH-dependence of A and B. Dashed lines in Fig. 3 represent the non-linear fittings. Although some simplifications could be achieved by considering just the ratio A/B, calculating this quotient from the fitted values of A and B has a relatively high error and values are not secure for further fittings. An iterative procedure was employed to obtain a single set of parameters (K_{12}/K_{11} and n_{app}) to satisfactorily fit the experimental results for both A and B (see the ESI†).

Fittings in Fig. 1–3 support the utility of the binding model to interpret the experimental results. The validity of the proposed model does not rely on the good fittings shown in Fig. 1, but on the capacity to explain the dependence of the parameters in eqn (14) on pH in terms of parameters with physicochemical meanings. In this sense, although it could be considered an oversimplified description of the binding phenomenon, the model keeps a minimal physical basis that allows performing physicochemical interpretations of the experimental results as discussed in the following section.

A.3. Physicochemical implications. The values of the binding equilibrium constants obtained from fittings allows quantifying the relative affinity (by K_{12}/K_{11}) of the divalent anionic phosphate species compared to singly charged phosphate, which results in five times higher values.

The discrimination of the relative binding tendencies of both phosphate species is difficult to achieve by straight experimental techniques due to the equilibriums involved and the fact that it is not possible to have just one of the phosphate species in solution in the physiologically relevant pH range. However, the simple binding model proposed here allows extraction of the binding tendencies (relative affinities) of the phosphate species bound to the amino groups from the experimental data for the zeta-potential (surface charge).

Several *in situ* spectroscopic techniques have been employed to study the nature of the bound phosphate species on metals, such as SERs[38] and FTIR.[39,40] More recent studies by employing SEIRAS on Au reported an apparent pK_a of about 7 that would suggest similar binding tendencies for HPO_4^{2-} and $H_2PO_4^{-}$.[41] However, the spectroscopic analysis also showed that the nature of the bound species is different from that in solution, owing to the strong interactions with the metal surface.[41]

Recently, molecular dynamics simulation results have been reported on the specific adsorption of phosphate anions on amino-terminated SAMs and the adsorption of cytochrome on these surfaces mediated by phosphates.[42] The simulation results indicate that phosphate anions effectively adsorb onto amino-terminated SAMs whereas chloride ions do not. They also show that HPO_4^{2-} has a stronger affinity to the surface than $H_2PO_4^{-}$ and the binding affinity is said to be mainly determined by their valence state.[43] Although the occurrence of salt bridges has been reported for this system, they have not taken into account the possibility of hydrogen-bonding type of interactions (see Section C).

The higher binding affinity of HPO_4^{2-} compared to $H_2PO_4^{-}$ can also be regarded as shifting of the dissociation equilibrium of bound phosphate species by interaction with the charged amino groups according to eqn (4). Taking into account the reported value of the second dissociation constant of phosphate $pK_{a2} = 7.2$ and the fitted values of the quotient $K_{12}/K_{11} = 5.1$, the apparent dissociation constant for the bound species is $pK_{app} = 6.5$. This value indicates that the interaction with charged amino groups induces a higher degree of dissociation of the bound phosphates as hypothesized in a previous work,[30] which translates into a higher charge state at around neutral pH. Scheme 2 depicts this idea. Similar results have been obtained for the case of the interaction of phosphatidic acid (a minor component of biological membranes) with charged amine species. Kooijman and co-workers have proved by ^{31}P-NMR that the interaction with charged primary and quaternary amines induces a higher dissociation degree of phosphatidic acid, changing its electrostatic charge from −1 to −2 at neutral pH.[44–46]

On the other hand, the determination of the values of the equilibrium constants allows estimation of the distribution of amino species under different pH and P_i concentration conditions. Fig. 4 shows the relative populations of amine moieties

8616 | *Phys. Chem. Chem. Phys.*, 2017, **19**, 8612–8620

This journal is © the Owner Societies 2017
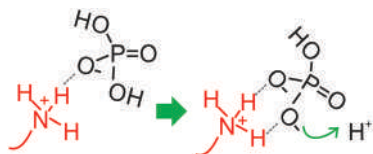
Scheme 2 The interaction with charged amine induces further proton dissociation on the phosphate anion.
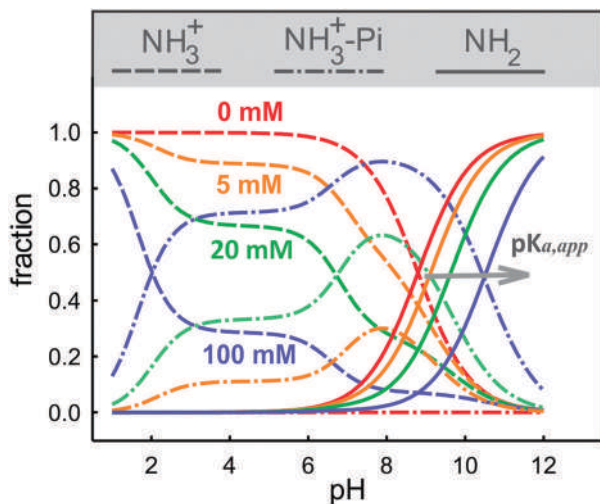

Fig. 4 Calculated distribution of amino species as a function of pH in the presence of different concentrations of phosphate as determined from the fitted values of the binding constants.

Fig. 5 Experimental zero-charge concentration (minimum phosphate concentrations required for charge inversion of the amino-functionalized surfaces), as a function of pH.

Fig. 6 Calculated values of the relative surface charge as a function of pH for different phosphate concentrations.

computed from the fitted values of model parameters. The shifting of the NH_2 distribution curve to a higher pH as the phosphate concentration increases is a consequence of the increase in the protonation degree induced by phosphates. Therefore, it can be said that in the presence of phosphates, the apparent pK_a of the amino groups increases.

The phenomenon of charge inversion can also be studied from the results of this simple binding model. According to eqn (16), the concentration that completely neutralizes the charge of the surface amino groups (zero-charge concentration) can be calculated as

$$[P_i]_0 = \frac{1}{A} = \frac{1 + 10^{-n_{app}(pH - pK_{app})}}{K_{11}\alpha_1 + K_{12}\alpha_2} \quad (18)$$

For concentrations higher than $[P_i]_0$, charge inversion occurs and surfaces become negative. Experimental values of zero-charge concentration as a function of pH are shown in Fig. 5. The phenomenon of charge inversion can also be analyzed from the values of ζ/ζ_+ calculated by employing the fitted binding constants. This ratio is the surface charge of the amino-functionalized surface relative to that of the completely proto-nated surface. These values are plotted in Fig. 6 as a function of pH for different phosphate concentrations. The analysis of these plots shows how the surface charge can be tuned by selecting the adequate pH and concentration conditions. This aspect is illustrated in the following section.
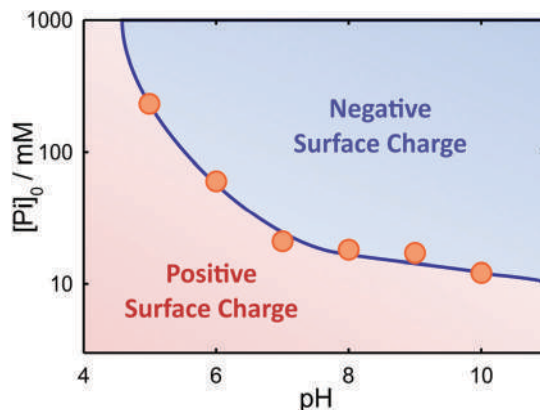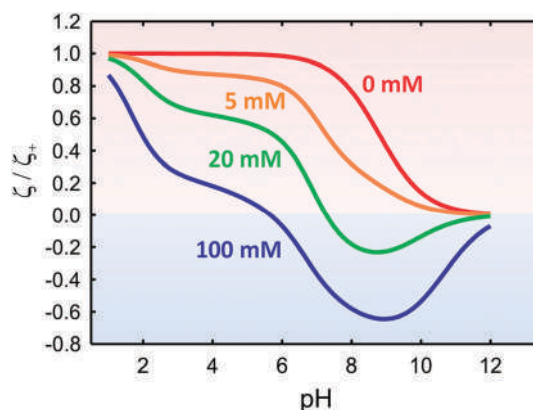
B. Protein adsorption and phosphate binding

The adsorption of glucose oxidase (GOx) upon amino-functionalized surfaces was employed as a case of study to illustrate the effect of phosphate anions on further interactions. The pH of the solutions for this study was maintained at 7.4 as it is considered as the physiological pH and, more remarkably, because it is the value of the phosphate-buffered saline (PBS: 10 mM P_i + 137 mM NaCl + 2.7 mM KCl), widely employed in biochemical and biological research. As GOx is a negative protein at this pH (isoelectric point pI = 4.2),[47] it is expected to adsorb onto the amino-functionalized surface mainly by electrostatic interactions.

The SPR response during the GOx adsorption on the Au/MPS/PAH sensor is presented in Fig. 7(A) for different concentrations of P_i (indicated in the figure) in 0.1 M KCl in 1 mM HEPES buffer. Clearly, the adsorption of GOx depends on the presence and concentration of phosphates in the solution. Whereas it strongly adsorbs in the absence of phosphates, it scarcely does when the P_i concentration is 50 mM. The addition of phosphate up to 1 mM produces a 30% decrease in protein adsorption even when it means just a 2% increment in the ionic strength of the solution. This implies that protein desorption cannot be ascribed to an ionic strength effect.

This journal is © the Owner Societies 2017

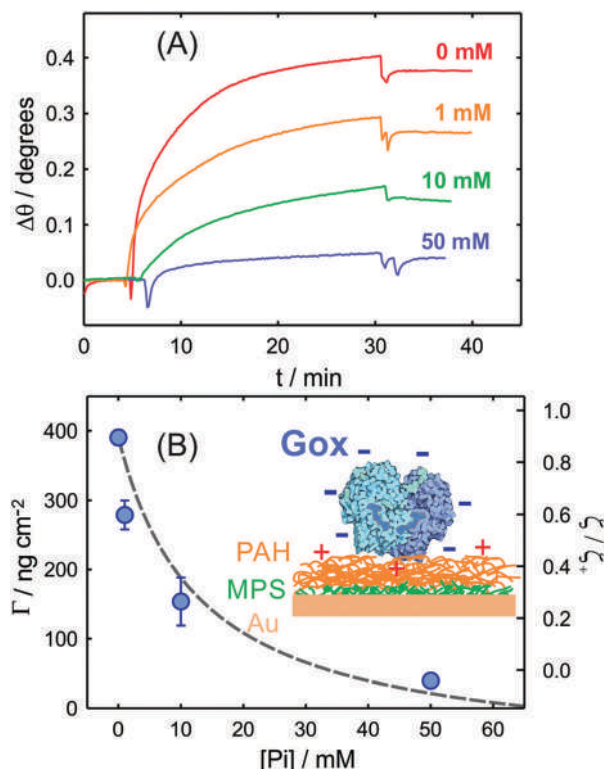Phys. Chem. Chem. Phys., 2017, **19**, 8612–8620 | 8617

Fig. 7 (A) Change in the minimum reflectivity angle of the SPR scan (measured at 785 nm) during the adsorption of GOx on Au/MPS/PAH sensors in the presence of different concentrations of phosphates in 0.1 M KCl in 1 mM HEPES buffer pH 7.4. Bars correspond to the std. deviation of 2 measurements. (B) Protein surface concentration as a function of the phosphate concentration. Dashed line corresponds to the quotient ζ/ζ_+ calculated at pH 7.4.

The remaining protein surface concentration, computed from $\Delta\theta$ and employing the instrumental factors and dn/dc of 0.182 cm^3 g^{-1} for globular proteins, is presented in Fig. 7(B) as a function of the phosphate concentration. In the same figure, the plot of the calculated values of the quotient ζ/ζ_+ at pH 7.4 was added for comparison. These results indicate that the changes in the adsorption of the negative protein correlate well with the calculated changes in the charge of the amino-functionalized surface induced by the binding of phosphate anions as calculated from the simple model presented here and the values of the binding constants determined from zeta-potential measurements. This good correlation reinforces the idea that the main effect is due to the inversion of the surface charge by the phosphate binding.

These results mark the relevance of the effect of phosphate binding on further interactions of amino-containing building blocks (proteins,[19] membranes,[13,17] polyelectrolytes,[18] etc.) as it critically modifies the electrostatic charges. On the other hand, these results show the importance of the reproduction of the *in vivo* phosphate concentrations in *in vitro* studies as it could markedly alter the interaction between different components and this may not only have structural but also functional consequences.[13] For example, our results show that the interaction of GOx with amino-containing surfaces would be critically

different if some of the so-called Good's buffers[48] are employed instead of PBS. Although this is an artificial system, the same implications hold for more biochemically relevant systems, such as the interaction of cytochrome *c* with the lipid components of the mitochondrial membrane.[13]

C. Specificity of binding: phosphates *vs.* other divalent anions

Although phosphates produce aggregates with soluble PAH more efficiently than other polyvalent anions,[30] recent computational studies affirm that the anion binding affinity to amino groups is mainly determined by its valence state.[43] On the other hand, the phosphate mediation of the adsorption of cytochrome *c* on amino-terminated SAMs reveals some specificity, but it is not undoubtedly due to the phosphate–amine interaction as it is known that cytochrome *c* also presents phosphate binding sites.[19]

To clarify the specificity of the interaction of surface amino groups with phosphates, we also studied comparatively the changes in the zeta-potential values of the SiO$_2$/PAH MPs in the presence of increasing concentrations of sulfate ($pK_{a2} = 1.99$) and oxalate ($pK_{a2} = 4.27$). These anions were employed as models of divalent anions as they are completely dissociated (valence -2) at pH 7 and then they would allow measurements of the electrostatic effect of this valence on the binding to amino units. The pH of the solutions was maintained at 7 for all the solutions. The results presented in Fig. 8 show that in the case of sulfate
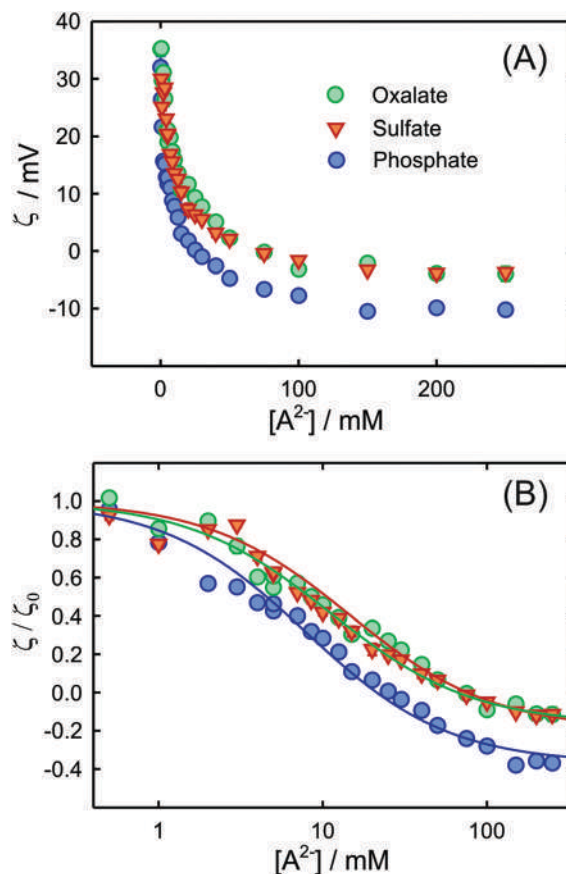

Fig. 8 Zeta-potential of SiO$_2$/PAH microparticles in the presence of different concentrations of divalent anions in 0.1 M KCl 1 mM in HEPES buffer, pH 7.

Table 1   Results of the fittings for different anions at pH 7

Anion	A (mM)	B (mM)	$[A^{-2}]_0$ (mM)	Final charge inversion (%)	K_B (mM^{-1})
Phosphate	0.048	0.106	21	45	0.082
Sulfate	0.013	0.075	77	17	0.013
Oxalate	0.015	0.084	67	18	0.015

and oxalate, there is also a decrease of the surface charge which is practically the same for both of them. However, the tendency is more marked when phosphate anions are present, which is more relevant when taking into account the fact that at this pH divalent species are only 40% of the total anion concentration. Furthermore, the binding of phosphates can produce a more marked charge inversion than the other divalent anions at pH 7 (Table 1). These observations can be quantitatively analyzed by employing the binding model developed above. The fittings of the experimental data to eqn (14) are also presented in Fig. 8. The values of the parameters of the fittings are presented in Table 1.

By taking into account the dissociation degree of the bound phosphate species (α_-) determined from the previous fittings (eqn (10)), the binding constant (K_B) for P$_i$ can be calculated (Table 1). Then, from the ratio $K_{12}/K_{11} = 5.1$, the specific binding constant of the divalent phosphate anion can be computed to be $K_{12} = 0.161$ mM^{-1} (eqn (7)). These results clearly show that the binding of phosphate anions is specific and cannot be explained only by electrostatic interactions as could be in the case of sulfate and oxalate (which present almost the same binding behavior). The binding constant for the divalent anion is one order of magnitude higher in the case of phosphates.

The specific binding of phosphates on amino-modified surfaces can be then explained by the presence of hydrogen bond interactions. The relative importance of this interaction translates into much higher affinity for phosphate species. The importance of hydrogen-bond interactions has been extensively recognized in the formation of aggregates between polyamines and phosphates,[31] as this type of interaction favors the formation of tridimensional networks.[36]

The relevance of hydrogen bond formation to the dissociation equilibrium of phosphatidic acid has also been studied by Kooijman and co-workers. They have shown that the hydrogen bond interaction with amine groups of phosphatidylethanolamine (a much more abundant membrane component), induces further dissociation of phosphatidic acid in membranes.[49,50] They have also proved that the interaction with protonated lysine and arginine also induces a higher dissociation degree of the phosphatidic acid at neutral pH. The effect is even higher than that produced by quaternary amines, which reinforces the idea that the effect of hydrogen bond formation is significant.[44] These studies motivated them to propose the so-called electrostatic/hydrogen bond switching model for the interaction of specific protein domains with this minor component of biological membranes.[44–46,50] According to this model, the proteins first randomly interact with other components of the membranes but as soon as an amine residue interacts with singly charged phosphatidic acid to form hydrogen bonds, it induces an additional deprotonation

to form a doubly charged species. The increment in the local negative charge then enhances the electrostatic attraction with the positively charged amine residue, reinforcing the interaction.[44,51] Our results indicate that a similar mechanism could be present in the interaction of charged amines with simple phosphate anions, as depicted in Scheme 2, which could explain the specificity and high affinity of this phenomenon.

Conclusions

The simple model presented here can satisfactorily describe the binding of phosphate anions to the amino-functionalized surfaces as it not only reproduces the qualitative trends but also allows the quantitative computation of meaningful parameters. In particular, this model allowed quantitatively determining the relative affinities of HPO$_4^{2-}$ and H$_2$PO$_4^-$ from the analysis of the influence of phosphate on the zeta-potential of amino-functionalized surfaces in a broad pH range. Furthermore, the interpretation of the experimental results in terms of the binding formalism allowed us to verify two related phenomena: in the presence of phosphates, the effective pK_a of amino groups increases, yielding a higher protonation degree at a given pH; and the interaction with protonated amino groups induces further proton dissociation of phosphates.

We have showed how the interplay of binding and proton dissociation equilibriums translates into a complex dependence of the surface effective charge on pH and phosphate concentration. As we exemplified for the case of GOx adsorption, the modulation of the charge state by phosphate binding has severe consequences on the interaction of amino surface groups with other components. In this sense, two main results deserve to be pointed out: phosphate–amine interaction is specific and it manifests in the millimolar range of phosphate concentration, which roughly coincides with the physiological range.

As P$_i$ concentrations vary in different tissues and even in different cellular compartments, it could be crucial to reproduce the in vivo P$_i$ concentrations in in vitro experiments even when phosphates are not directly involved in the studied process as they may alter the interactions of surface amino groups in different proteins and cellular components. Furthermore, the indiscriminate use of PBS as a buffer in biochemical studies should be thoroughly revised as it could strongly modify the structural, and also the functional, role of amino surface groups and may deeply affect the extrapolation of the results to in vivo conclusions.

Notes and references

1 *Manipulation of Nanoscale Materials: An Introduction to Nanoarchitectonics*, ed. K. Ariga, Royal Society of Chemsitry, Cambridge, 2012.

2 *Hydrogen Bonded Supramolecular Materials*, ed. Z.-T. Li and L.-Z. Wu, Springer-Verlag, Heidelberg, 2015.

3 J. Simon and P. Bassoul, *Design of Molecular Materials: Supramolecular Engineering*, John Wiley & Sons, Chichester, 2000.

4 J. Li, Q. He and X. Yan, *Molecular Assembly of Biomimetic Systems*, VCH-Wiley, Weinheim, 2011.

5 L. Jiang and L. Feng, *Bioinspired intelligent nanostructured interfacial materials*, World Scientific Publishing Company, Singapore, 2010, vol. 38.

6 C. S. S. R. Kumar, *Biomimetic and Bioinspired Nanomaterials*, VCH-Wiley, Weinheim, 2010.

7 B. Honig and A. Nicholls, *Science*, 1995, **268**, 1144–1149.

8 A. W. Ritchie and L. J. Webb, *J. Phys. Chem. B*, 2015, **119**, 13945–13957.

9 D. B. Kitchen, H. Decornez, J. R. Furr and J. Bajorath, *Nat. Rev. Drug Discovery*, 2004, **3**, 935–949.

10 M. Rabe, D. Verdes and S. Seeger, *Adv. Colloid Interface Sci.*, 2011, **162**, 87–106.

11 J. J. Gray, *Curr. Opin. Struct. Biol.*, 2004, **14**, 110–115.

12 O. Gerlits, T. Wymore, A. Das, C. H. Shen, J. M. Parks, J. C. Smith, K. L. Weiss, D. A. Keen, M. P. Blakeley, J. M. Louis, P. Langan, I. T. Weber and A. Kovalevsky, *Angew. Chem., Int. Ed.*, 2016, **55**, 4924–4927.

13 D. A. Capdevila, W. A. Marmisolle, F. Tomasina, V. Demicheli, M. Portela, R. Radi and D. H. Murgida, *Chem. Sci.*, 2015, **6**, 705–713.

14 D. Alvarez-Paggi, D. F. Martín, P. M. DeBiase, P. Hildebrandt, M. A. Martí and D. H. Murgida, *J. Am. Chem. Soc.*, 2010, **132**, 5769–5778.

15 M. Y. Tsai, W. Zheng, D. Balamurugan, N. P. Schafer, B. L. Kim, M. S. Cheung and P. G. Wolynes, *Protein Sci.*, 2016, **25**, 255–269.

16 J. J. Richardson, M. Bjornmalm and F. Caruso, *Science*, 2015, **348**, aaa2491.

17 W. A. Marmisolle, D. A. Capdevila, E. De Llave, F. J. Williams and D. H. Murgida, *Langmuir*, 2013, **29**, 5351–5359.

18 J. Irigoyen, S. E. Moya, J. J. Iturri, I. Llarena, O. Azzaroni and E. Donath, *Langmuir*, 2009, **25**, 3374–3380.

19 D. A. Capdevila, W. A. Marmisollé, F. J. Williams and D. H. Murgida, *Phys. Chem. Chem. Phys.*, 2013, **15**, 5386–5394.

20 M. G. M. G. Penido and U. S. Alon, *Pediatr. Nephrol.*, 2012, **27**, 2039–2048.

21 J. J. Scialla and M. Wolf, *Nat. Rev. Nephrol.*, 2014, **10**, 268–278.

22 T. P. M. Akerboom, H. Bookelman, P. F. Zuurendonk, R. van der Meer and J. M. Tager, *Eur. J. Biochem.*, 1978, **84**, 413–420.

23 N. Kröger, S. Lorenz, E. Brunner and M. Sumper, *Science*, 2002, **298**, 584–586.

24 N. Kröger, R. Deutzmann, C. Bergsdorf and M. Sumper, *Proc. Natl. Acad. Sci. U. S. A.*, 2000, **97**, 14133–14138.

25 L. D'Agostino and A. Di Luccia, *Eur. J. Biochem.*, 2002, **269**, 4317–4325.

26 L. D'Agostino, M. di Pietro and A. Di Luccia, *FEBS J.*, 2005, **272**, 3777–3787.

27 A. Di Luccia, G. Picariello, G. Iacomino, A. Formisano, L. Paduano and L. D'Agostino, *FEBS J.*, 2009, **276**, 2324–2335.

28 M. Sumper, *Angew. Chem., Int. Ed.*, 2004, **43**, 2251–2254.

29 E. Brunner, K. Lutz and M. Sumper, *Phys. Chem. Chem. Phys.*, 2004, **6**, 854–857.

30 W. J. Dressick, K. J. Wahl, N. D. Bassim, R. M. Stroud and D. Y. Petrovykh, *Langmuir*, 2012, **28**, 15831–15843.

31 W. A. Marmisollé, J. Irigoyen, D. Gregurec, S. Moya and O. Azzaroni, *Adv. Funct. Mater.*, 2015, **25**, 4144–4152.

32 Y. Huang, P. G. Lawrence and Y. Lapitsky, *Langmuir*, 2014, **30**, 7771–7777.

33 P. G. Lawrence and Y. Lapitsky, *Langmuir*, 2015, **31**, 1564–1574.

34 W. Stöber, A. Fink and E. Bohn, *J. Colloid Interface Sci.*, 1968, **26**, 62–69.

35 K. Itano, J. Choi and M. F. Rubner, *Macromolecules*, 2005, **38**, 3450–3460.

36 K. Lutz, C. Gröger, M. Sumper and E. Brunner, *Phys. Chem. Chem. Phys.*, 2005, **7**, 2812–2815.

37 W. A. Marmisollé, M. I. Florit and D. Posadas, *J. Electroanal. Chem.*, 2014, **734**, 10–17.

38 G. Niaura, A. K. Gaigalas and V. L. Vilker, *J. Phys. Chem. B*, 1997, **101**, 9250–9262.

39 M. Weber, F. C. Nart and I. R. de Moraes, *J. Phys. Chem.*, 1996, **100**, 19933–19938.

40 M. Weber and F. C. Nart, *Electrochim. Acta*, 1996, **41**, 653–659.

41 M. Yaguchi, T. Uchida, K. Motobayashi and M. Osawa, *J. Phys. Chem. Lett.*, 2016, **7**, 3097–3102.

42 C. Peng, J. Liu, Y. Xie and J. Zhou, *Phys. Chem. Chem. Phys.*, 2016, **18**, 9979–9989.

43 C. Peng, J. Liu, Y. Xie and J. Zhou, *Phys. Chem. Chem. Phys.*, 2016, **18**, 9979–9989.

44 E. E. Kooijman, D. P. Tieleman, C. Testerink, T. Munnik, D. T. S. Rijkers, K. N. J. Burger and B. De Kruijff, *J. Biol. Chem.*, 2007, **282**, 11356–11364.

45 E. E. Kooijman and K. N. J. Burger, *Biochim. Biophys. Acta, Mol. Cell Biol. Lipids*, 2009, **1791**, 881–888.

46 D. H. Mengistu, E. E. Kooijman and S. May, *Biochim. Biophys. Acta, Biomembr.*, 2011, **1808**, 1985–1992.

47 J. H. Pazur and K. Kleppe, *Biochemistry*, 1964, **3**, 578–583.

48 N. E. Good, G. D. Winget, W. Winter, T. N. Connolly, S. Izawa and R. M. M. Singh, *Biochemistry*, 1966, **5**, 467–477.

49 E. E. Kooijman, K. M. Carter, E. G. van Laar, V. Chupin, K. N. J. Burger and B. de Kruijff, *Biochemistry*, 2005, **44**, 17007–17015.

50 J. J. Shin and C. J. Loewen, *BMC Biol.*, 2011, **9**, 85.

51 U. Kwolek, D. Jamróz, M. Janiczek, M. Nowakowska, P. Wydro and M. Kepczynski, *Langmuir*, 2016, **32**, 5004–5018.